*Title page

Individual differences in structural and functional connectivity predict speed of emotion discrimination

Lars Marstaller[1,2], Hana Burianová[1,3], and David C. Reutens[1]

[1]Centre for Advanced Imaging, University of Queensland, Brisbane, Australia

[2]ARC Science of Learning Research Centre, University of Queensland, Brisbane, Australia

[3]Department of Psychology, Swansea University, Swansea, United Kingdom

Correspondence should be addressed to:

Lars Marstaller, PhD

Centre for Advance Imaging

University of Queensland

QLD 4072, AUSTRALIA

l.marstaller@uq.edu.au

Pages: 25

Figures: 5

Highlights

- Discrimination speed of angry and fearful faces related to separate networks.
- Angry faces are discriminated faster by extended emotional face processing network.
- Fearful faces are discriminated faster by cortical visual-attentional regions.
- Discrimination speed of angry but not fearful faces associated with right amygdala.
- Integrity of inferior longitudinal fasciculus improves threat discrimination speed.

Abstract

In social interactions, individuals who are slower at differentiating between facial expressions signalling direct and indirect threat might be at a serious disadvantage. However, the neurobiological underpinnings of individual differences in face processing are not yet fully understood. The aim of this study was to use multimodal neuroimaging to investigate how the speed of emotion recognition is related to the structural and functional connectivity underlying the differentiation of direct and indirect threat displays. Our results demonstrate that individuals, who are faster at discriminating angry faces, engaged areas of the extended emotional system more strongly than individuals with slower reaction times, showed higher white matter integrity in the inferior longitudinal fasciculus, as well as stronger functional connectivity with the right amygdala. In contrast, individuals, who were faster at discriminating fearful faces, engaged visual-attentional regions outside of the face processing network more strongly than individuals with slower reaction times, showed higher white matter integrity in the inferior longitudinal fasciculus, as well as reduced functional connectivity with the right amygdala. Our findings suggest that the high survival value of rapid and appropriate responses to threat has defined but separate neurobiological correlates for angry and fearful facial expressions.

Keywords: emotion discrimination; structural-functional connectivity; individual differences

1. Introduction

Rapid and accurate discrimination of facial expressions of emotion is important for preparing adequate and timely responses in social interactions (Cizek & Kalaska, 2010). Rapid discrimination is particularly important for facial expressions displaying anger and fear, as these emotions signal direct and indirect threat respectively, which might require an immediate fight-or-flight response (Bannerman et al., 2009; Hansen & Hansen, 1988; Lo & Cheng, 2015; Whalen et al., 2001). Previous research has shown that the ability to rapidly discriminate between emotional facial expressions signalling threat depends on the core face-processing network, including inferior occipital gyrus, superior temporal sulcus, and fusiform gyrus, as well as the extended emotional system centered on the amygdala (Haxby et al. 2002; Rossion et al., 2003; Gobbini & Haxby, 2007). During the conscious recognition of threatening emotional facial expressions, the core network and the extended emotional system interact through bidirectional functional connections between the amygdala and the fusiform gyrus (Herrington et al., 2011; Wang et al., 2016). Functional connectivity between fusiform gyrus and amygdala, together with the ability to discriminate emotions depend on white matter pathways within the inferior longitudinal fasciculus (Kleinhans et al., 2008; Koldewyn et al., 2014). This structural-functional relationship allows the amygdala to exert top-down control on the ventral visual pathway during the perception of threat-signalling facial expressions (Amaral, Behniea & Kelly, 2003; Villeumier et al., 2003; De Gelder et al., 2014). Thus, this evidence suggests that rapid discrimination of threat-related emotional facial expressions crucially depends on the functional and structural connectivity between the amygdala and fusiform gyrus and that individuals with less efficient structural and functional connectivity may be at a disadvantage in threat-

related social interactions. However, to date, no study has investigated whether the functional and structural connectivity between the amygdala and fusiform gyrus affects the speed of emotion discrimination in healthy adults.

The objective of this study was to investigate whether individual differences in structural integrity and functional connectivity between the core and extended emotional face-processing networks would predict the speed of conscious emotion discrimination for angry and fearful facial expressions. In particular, we were interested in the three-way relation between structural connectivity, functional connectivity, and behaviour during an emotion discrimination task that required participants to match facial expressions of fear or anger. As an indicator of structural connectivity, we assessed the white matter integrity of the inferior longitudinal fasciculus (ILF), which constitutes the major white matter pathway along the ventral visual processing stream, mediating the interactions between the amygdala and the fusiform gyrus during face processing (Catani et al., 2003; Thomas et al., 2009). As an indicator of functional connectivity, we used a seed-based approach and covaried functional activity within the amygdala with task-related activity across the whole brain. As an indicator of behaviour, we measured reaction times of emotion discrimination. Based on previous studies, which show that angry and fearful faces are identified equally fast and that processing of both emotions engages the core and extended face-processing networks (De Sonneville et al., 2002; Whalen et al., 2001), we hypothesized that, as a group, participants would (i) be equally fast to match angry and fearful faces and (ii) engage the core and extended face processing networks for both facial expressions. Based on the assumption that the discrimination of different emotional expressions requires the interaction between the amygdala and fusiform gyrus (Herrington et al., 2011; Wang et al., 2016), we further hypothesized that (iii)

for both angry and fearful facial expressions, individuals who discriminate emotions more rapidly would also have better white matter integrity in the ILF and increased functional connectivity within and between the core and extended face-processing networks. More specifically, we hypothesized that shorter reaction times should correlate with higher FA values as well as connectivity values in the face processing network.

2. Methods

2.1 Participants

28 right-handed adults (14 females, mean age = 26.3 years, age range = 21-34 years) with normal or corrected to normal vision gave written consent to take part in the experiment, which was approved by the Human Ethics Research Committee of the University of Queensland. All participants were screened for neuropsychological disorders, brain damage, and substance abuse. Images were acquired with a Siemens Magnetom Trio 3T (Siemens Healthcare, Erlangen, Germany) and a standard 32-channel head coil at the Centre for Advanced Imaging, University of Queensland.

2.2 Experimental Procedure

Participants took part in an emotion-matching task adapted from the paradigm described in Hariri et al. (2000). During each trial, three images were presented, one in the top and two in the bottom half of the screen using Presentation software (Neurobehavioral Systems, Inc.). One of the bottom two images was identical to the top image and participants were asked to identify the image in the bottom half of the screen that matched the top image by pressing the one of two buttons associated with the left and right image. Images either showed black elliptical shapes angled at 45º or

315º (shapes condition) or facial expressions with a target of angry (angry condition) or fearful facial expressions (fearful condition). During presentation of facial expressions, all pictures were of the same model and always included one fearful and one angry facial expression presented in the bottom row, which makes the two facial expression conditions directly comparable. Reaction times were measured and data from individual trials was removed from the behavioural analysis if they constituted outliers, i.e., a reaction time shorter than 350 ms or longer than 1800 ms.

Image stimuli consisted of 24 pictures selected from the Radboud Faces Database (http://www.socsci.ru.nl:8180/RaFD2/RaFD). In each picture, a trained model (young adult Caucasian males and females) displayed either a fearful or an angry facial expression with direct gaze (Langner et al., 2010). Control stimuli consisted of black ellipses angled at 45º or 315º generated by Presentation software. Images were presented in 6 blocks (3 blocks of shapes, 3 blocks of faces), each containing 6 trials. The presentation order of blocks was randomized. At the beginning of each block, an instruction was presented for 3s to either "match the faces" or to "match the shapes". In each trial, the images were presented for 2s followed by a fixation cross for 1s.

Due to a technical error, the behavioural accuracy of the participants' responses was not recorded. Observations of participants' responses during the task suggested that behavioural accuracy was at ceiling and that accuracy would not be an important factor in assessing the relation between behaviour, structure, and function. To confirm this observation, we subsequently tested the same paradigm behaviourally in a separate sample of 28 young, right-handed adults (mean age = 22 years, age range = 18-30 years, 19 females). As predicted, participants' accuracies showed a ceiling effect for each of the three stimulus types: angry faces group mean score = 0.96, SD =

0.04; fearful faces group mean score = 1.0, SD = 0.0; and shapes group mean score = 0.94, SD = 0.09. To ensure comparability between the two groups, we further compared their reaction times. A 2 x 3 mixed-design ANOVA of the dependent variable reaction time with a fixed effects factor group (first, second) and a random effects factor stimulus (angry, fearful, shapes) yielded a significant factor of group ($F(1) = 40.167$, $p < 0.001$) and a significant factor of stimulus ($F(2) = 20.603$, $p < 0.001$), but no interaction between factors. Using only data from the second group, two-sided t-tests of the reaction times to different stimulus types showed significantly faster responses to shapes than to angry and fearful facial expressions (both $t(27) > 6.4$, both $p < 0.001$) but not between facial expressions ($t(27) = 0.5$, $p = 0.7$). These results replicate the results reported below for the first group although participants in the second group were overall faster across all stimulus types (significant main effect of the factor group). This group difference can be attributed to the different testing conditions because the first group was tested in the MRI whereas the second group was tested in a behavioural laboratory. Taken together, these results confirm that reaction time but not accuracy should be considered an important factor when investigating the relation between behaviour, structure, and function during the emotion-matching task.

2.3 Image Acquisition

For each participant, a T1-weighted volumetric anatomical MRI was acquired with the following parameters: 176 slices sagittal acquisition MP2RAGE; $1mm^3$ isotropic volume; repetition time (TR) = 4000 msec; echo time (TE) = 2.89 msec; flip angle = 6°; FOV = 256 mm, GRAPPA acceleration factor = 3. Functional images were acquired using a T2*-weighted echo-planar image pulse sequence with the

following parameters: 45 slices; voxel size = 2.5 x 2.5 x 2.7 mm; TR = 3000 msec; TE = 30 msec; FOV = 192 mm; flip angle = 90°. Diffusion-weighted images with a high angular resolution (HARDI) were acquired for each participant using a fast echo-planar sequence with the following parameters: b1-value = 3000 s/mm^2; 64 gradient directions; TR = 8600 msec; TE = 109 msec; FOV = 240 mm; 60 slices; voxel size = 2.3 mm isotropic; GRAPPA acceleration factor = 2.

2.4 fMRI Preprocessing & Whole-Brain Analysis

Brain activation was assessed using the blood oxygenation level dependent (BOLD) effect (Ogawa et al., 1990) with optimal contrast. For functional analysis, T2*-weighted images were preprocessed with Statistical Parametric Mapping software (SPM8; http://www.fil.ion.ucl.ac.uk/spm). Images were realigned to a mean image to correct for head motion and then spatially normalized into standard stereotaxic space with voxel size of 2 mm^3, using the Montreal Neurological Institute (MNI) template. Head movement and rotation did not exceed 1 mm or 1.5º and no dataset had to be excluded from the analysis. Finally, the functional images were spatially smoothed with a 6-mm full width half maximum Gaussian kernel.

Following preprocessing, images were submitted to whole-brain analysis using PLS software (PLS, http://www.rotman-baycrest.on.ca/index.php?section=84). PLS analysis proceeds in several steps (McIntosh et al., 1996, 2004; Krishnan et al., 2011). First, data from individual trials and participants are sorted by condition and collated into a single data matrix and a second matrix containing task design (for task-PLS) as well as covariates of interest (seed-PLS) is created. Second, the data and covariate matrices are mean-centered and normalized. Third, a covariance matrix is created from the dot product of the data and covariates matrices. Fourth, PLS uses

singular value decomposition - a form of principal components analysis – to identify brain activity patterns related to task conditions (task PLS) and task conditions as well as seed values (seed PLS). Since PLS analyzes the data in a single analytical step, no corrections for multiple comparisons are necessary. Singular value decomposition yields latent variables that relate to the largest dimensions of variation within the data. Each latent variable consist of a pattern of brain activity, a singular value, and a matrix of loadings that indicate how each pattern relates to the task design and the seed values. Fifth, PLS assesses the reliability of the brain activity patterns at each voxel using a bootstrap estimation of the standard error with 100 iterations. All brain activity patterns were thresholded at a bootstrap ratio of 2 as this equates to a p-value of < 0.05. Sixth, PLS calculates a brain score for each experimental condition and each participant, which indicates how strong a pattern is represented in the experimental sample (McIntosh et al., 2004). Brain scores therefore represent individual differences.

2.5 White Matter Analysis

Structural connectivity was assessed using MRtrix3 software (https://github.com/MRtrix3/) and tools from the FMRIB Software Library (FSL 5.0.6; http://fsl.fmrib.ox.ac.uk/fsl/fslwiki/). HARDI images were first corrected for motion and eddy current artefacts using *eddy_correct*, after which vectors were reoriented using *fdt_rotate_bvecs* (Graham, Drobnjak & Zhang, 2016). Then, a brain mask was created from the corrected b0 image using *fslroi* and skull-stripped using *bet* (Smith, 2002). Tensors were fitted using *dwi2tensor*, and fractional anisotropy (FA) values were computed for each voxel using *tensor2metric* (Veraart et al., 2013). Next, the DWI response function was estimated using *dwi2response* and the fiber

orientation distribution (FOD), which was derived using constrained spherical deconvolution (CSD) with harmonic order 8 as implemented in *dwi2fod* (Tournier et al., 2004, 2007).

For tractography, each individual's T1-weighted image was first segmented using FSL's *first* to derive individual masks for gray matter and cerebro-spinal fluid (CSF; Patenaude et al., 2011). Then, masks for left and right amygdala, as well as left and right fusiform gyrus were defined as anatomical regions of interest using the AAL atlas and masked using individual gray matter masks (Tzourio-Mazoyer et al., 2002). All masks were transformed into individual diffusion space using *flirt* (Jenkinson & Smith, 2001; Jenkinson et al., 2002). Unidirectional probabilistic streamlines between amygdala seed masks and fusiform gyrus inclusion masks were computed for each hemisphere using *tckgen*, the FODs derived from CSD, an exclusion mask derived from each individual's CSF, and the iFOD2 algorithm with a step size of 1.15 and a cut-off of 0.15 (Tournier et al., 2010, 2012). After visual inspection, streamlines were converted to track-density images with *tckmap*, thresholded using *mrthreshold*, binarized with *fslmaths*, and used as masks to extract the mean values for each individual from the FA images using *fslstats* (Calamante et al., 2010).

2.6 Structure-Function-Behaviour Analysis

To assess the relation between reaction time, ILF FA values, and amygdala functional connectivity, average time-courses of seed regions in left and right dorsal amygdala were first extracted from each individual using a 5-mm sphere centered at MNI coordinates [-20 -8 -12] and [22 -6 -12]. The coordinates were chosen based on a priori anatomical information about the location of the left and right amygdala as well as the results of the whole-brain analysis, where the coordinates represent peak

amygdala activations differentiating the processing of fearful and angry faces from shapes. Then, the mean reaction times, mean ILF FA values, and functional seed values were correlated with each participant's whole-brain activity and submitted to seed PLS analysis (Krishnan et al., 2011). In seed PLS analysis, the results display the Pearson product-moment correlation coefficient between brain scores of the LV and the reaction times, ILF FA values, and amygdala functional seed values for each condition (Marstaller et al., 2015). As a consequence, these correlations reflect individual differences in the three-way relation between structure, function, and behavior.

3. Results

3.1 Reaction times

Repeated measures two-sided t-tests revealed that participants responded significantly faster to shapes (mean RT = 899.14 ms, SD = 163.89 ms) than angry (mean RT = 1096.11 ms, SD = 170.78 ms; $t(27) = 6.3$, $p < 0.001$) and fearful faces (mean RT = 1065.88 ms, SD = 153.61 ms; $t(27) = 5.8$, $p < 0.001$). There was no significant difference in reaction times between angry and fearful faces ($t(27) = 1.3$, $p = 0.21$; see Figure 1A). Reaction times for angry and fearful faces were highly correlated ($r = 0.7$).

3.2 ILF white-matter integrity

Group-mean FA-values were 0.42 (SD = 0.03) for the left and 0.41 (SD = 0.06) for the right ILF. A two-sided repeated measures t-test showed no significant differences between the two hemispheres ($t(27) = 1.5$, $p = 0.13$; see Figure 1B).

(INSERT FIGURE 1 HERE)

3.3 Whole-brain task-related functional activity

PLS analysis resulted in two significant whole-brain activity patterns. The first pattern of activity differentiated the control condition (shapes) from face presentations and demonstrated a shared activation pattern for angry and fearful expressions. Angry and fearful faces were associated with increased activity in the core and extended emotional face processing system, including bilateral inferior occipital gyrus, fusiform gyrus, and dorsal amygdala (see cool colours in Figure 2). Presentation of shapes resulted in greater activity in posterior parietal cortices (see warm colours in Figure 2; see Table 1).

(INSERT FIGURE 2 HERE)

The second significant pattern of activity differentiated angry from fearful faces. For angry faces, the pattern showed increased activity in the right orbitofrontal cortex, left caudate nucleus, and middle frontal cortex, as well as in areas commonly associated with semantic processing (right hippocampus and middle temporal gyrus; Binder et al., 2009), salience detection (anterior cingulate cortex; Critchley, 2005), and bottom-up attention (right ventrolateral prefrontal cortex and right supramarginal gyrus; Fox et al., 2006; see warm colours in Figure 3). For fearful faces, the pattern showed increased activity in the right ventral amygdala, fusiform gyrus, and left pallidum (see cool colours in Figure 3; see Table 2).

(INSERT FIGURE 3 HERE)

3.4 Three-way relation between reaction time, ILF integrity, and amygdala functional connectivity

PLS analysis revealed two significant whole-brain patterns of amygdala functional connectivity that showed a different relation between functional connectivity, behaviour and ILF white matter integrity for angry and fearful faces. During perception of angry facial expressions, a set of limbic-temporal regions was functionally connected to the right (r = 0.37) but not the left amygdala (r = -0.028). This functional network was negatively correlated with reaction times (r = -0.72), but positively correlated with FA values of the left (r = 0.45) and right ILF (r = 0.37) and included bilateral hippocampus, brainstem, and the right temporal pole (see Figure 4). These results therefore show that individuals, who were faster at identifying angry faces, engaged this extended amygdala network more strongly, had better connectivity with the right amygdala, and a higher ILF white matter integrity bilaterally. Individual differences in the three-way relation between behaviour, white matter integrity, and functional connectivity are displayed as scatter plots that indicate how much each factor correlated with the depicted pattern of activity across the sample (see Figure 4).

(INSERT FIGURE 4 HERE)

A second frontal-parietal-occipital network showing negative functional connectivity with the right (r = -0.53) but not the left amygdala (r = -0.15) was engaged during perception of fearful facial expressions. This functional network was

negatively correlated with reaction time (r = -0.37) but positively with FA values of the left (r = 0.3) and right ILF (r = 0.51) and included bilateral lingual gyrus, precuneus, middle and superior frontal gyrus, supramarginal gyrus, and precentral gyrus meaning that individuals, who were faster at differentiating fearful faces, engaged this fronto-parietal-occipital network more strongly, had lower connectivity with the right amygdala, and a higher ILF white matter integrity bilaterally. Individual differences in the three-way relation between behaviour, white matter integrity, and functional connectivity are displayed as scatter plots that indicate how much each factor correlated with the depicted pattern of activity across the sample (see Figure 5).

(INSERT FIGURE 5 HERE)

5. Discussion

In social interactions, individuals who are slower at distinguishing between facial expressions signalling direct and indirect threat might be at a serious disadvantage. However, the neurobiological underpinnings of individual differences in face processing are not yet fully understood. The aim of this study was to investigate how the speed of emotion recognition is related to the structural and functional connectivity underlying the differentiation of direct and indirect threat displays. The analysis of the three-way relation between behaviour, structure, and function underlying the core and extended systems for angry and fearful face processing revealed behaviourally relevant individual differences. Individuals who were faster at identifying angry faces engaged areas of the extended emotional system more strongly than individuals with slower reaction times. These faster individuals further showed higher white matter integrity in the ILF and stronger functional

connectivity with the right amygdala, suggesting that an efficient structural and functional connectivity between the core and extended emotional systems is crucial for the rapid processing of facial expressions signalling direct threat. This finding implicates that the high survival value of rapid and appropriate responses to direct threat has a defined neurobiological correlate.

With respect to fearful faces that signal indirect threat, our results showed that individuals who were faster at discriminating fearful faces also had more intact white matter in the ILF but less functional connectivity between the face processing network and the amygdala. Those faster individuals engaged more regions outside of the face processing network related to attention and visual processing, suggesting that the processing speed of facial expressions signalling indirect threat profits from the recruitment of additional visual-attentional systems, which are engaged in searching for novel cues that help reduce the ambiguity associated with indirect threat expressions (Whalen et al., 2001; Phelps, Ling, & Carrasco, 2005). In contrast to direct threat, the rapid recognition of indirect threat, therefore, seems to depend less on the cortical face-processing network and instead might rely more on a subcortical pathway (Villeumier et al., 2003). In addition, individual differences in the rapid recognition of indirect threat displays seem to directly translate into the ability to gather additional information that reduces the ambiguity associated with fearful facial expressions, and individuals who rapidly reduce ambiguity might profit from higher white matter integrity in the ILF along the ventral visual stream.

The whole-brain results confirm previous findings by demonstrating the engagement of the core face-processing network, which consists of inferior occipital and fusiform gyrus and the extended emotional system centered around the amygdala, for both angry and fearful faces (Adolphs, 2002; Haxby et al. 2002; LaBar et al.,

2003; Gobbini & Haxby, 2007). The results further show that the dorsal amygdala and fusiform gyrus are engaged during the perception of both angry and fearful faces, which is in accordance with previous findings demonstrating increased vigilance during perception of threat (Davis & Whalen, 2001; Williams et al., 2001). The absence of activity in the superior temporal sulcus and premotor cortices in our data is possibly related to the static stimuli used in this experiment (Grèzes, Pichon & de Gelder, 2007; Said, Haxby & Todorov, 2011). Perception of angry faces additionally activated cortical regions associated with evaluative processing, such as the salience (Menon & Uddin, 2010; Pichon, de Gelder & Grèzes, 2012) and ventral attention networks (Corbetta & Shulman, 2002), as well as regions associated with memory processing (Haxby et al., 1996; Frey & Petrides, 2003; Tsukiura & Cabeza, 2008). This finding suggests that angry faces might engage cortical regions related to evaluative, contextual processing more strongly than fearful faces, perhaps because anger directs attention towards the angry individual, whereas fear directs attention towards the ambiguous cause of the threat (Grosbras & Paus, 2006; Pichon, de Gelder & Grèzes, 2009). Fearful faces additionally engaged the amygdala and fusiform gyrus, which is in line with previous findings and suggests increased processing of fearful compared to angry facial expressions within regions of the core and extended emotional faces processing systems (Whalen et al., 2001). Perception of fearful faces further engaged the left globus pallidum, which might be related to the initiation of a fight-or-flight response (Korzeniewska, Kasicki & Zagrodzka, 1997; Grèzes & Dezecache, 2014).

In sum, our results extend our current knowledge about the networks involved in the processing of emotional facial expressions by demonstrating that individual differences in the structural and functional connectivity within and between the core

and extended emotional face-processing systems affect the speed at which emotional faces are discriminated. The associated adaptive value of efficient structural and functional connectivity between the core and extended emotional face-processing systems points towards a neurobiological cause for individual differences in social interactions. As a consequence, genetic and environmental factors that influence the development and age-related degeneration of structural and functional connectivity underlying emotional face discrimination might determine an individual's success in responding to threat in social interactions and hence impart a high survival value (Cohen Kadosh, 2011; Scherf et al., 2014; Shaw et al., 2016).

Acknowledgements

This work was funded by the Australian Research Council Special Research Initiative: Science of Learning Research Centre (project number SR120300015).

References

Adolphs R (2002) Recognizing emotion from facial expressions: psychological and neurological mechanisms. Behav Cogn Neurosci Rev. 1: 21-62.

Amaral DG, Behniea H, Kelly JL (2003) Topographic organization of projections from the amygdala to the visual cortex in the macaque monkey. Neuroscience. 118: 1099-120.

Bannerman RL, Milders M, de Gelder B, Sahraie A (2009) Orienting to threat: faster localization of fearful facial expressions and body postures revealed by saccadic eye movements. Proc Biol Sci. 276: 1635-41.

Binder JR, Desai RH, Graves WW, Conant LL (2009) Where is the semantic system? A critical review and meta-analysis of 120 functional neuroimaging studies. Cereb Cortex. 19: 2767-96.

Calamante F, Tournier JD, Jackson GD, Connelly A (2010) Track-density imaging (TDI): super-resolution white matter imaging using whole-brain track-density mapping. Neuroimage. 53: 1233-43.

Catani M, Jones DK, Donato R, Ffytche DH (2003) Occipito-temporal connections in the human brain. Brain. 126: 2093-107.

Cisek P, Kalaska JF (2010) Neural mechanisms for interacting with a world full of action choices. Annu Rev Neurosci. 33: 269-98.

Cohen Kadosh K (2011) What can emerging cortical face networks tell us about mature brain organisation? Dev Cogn Neurosci. 1: 246-55.

Corbetta M, Shulman GL (2002) Control of goal-directed and stimulus-driven attention in the brain. Nat Rev Neurosci. 3: 201-15.

Critchley HD (2005) Neural mechanisms of autonomic, affective, and cognitive integration. Journal of Comparative Neurology. 493: 154-66.

de Gelder B, Terburg D, Morgan B, Hortensius R, Stein DJ, van Honk J (2014) The role of human basolateral amygdala in ambiguous social threat perception. Cortex. 52: 28-34.

De Sonneville LM, Verschoor CA, Njiokiktjien C, Op het Veld V, Toorenaar N, Vranken M (2002) Facial identity and facial emotions: speed, accuracy, and processing strategies in children and adults. J Clin Exp Neuropsychol. 24: 200-13.

Fox MD, Corbetta M, Snyder AZ, Vincent JL, Raichle ME (2006) Spontaneous neuronal activity distinguishes human dorsal and ventral attention systems. Proc Natl Acad Sci. 103: 10046-51.

Frey S, Petrides M (2003) Greater orbitofrontal activity predicts better memory for faces. Eur J Neurosci. 17: 2755-8.

Gobbini MI, Haxby JV (2007) Neural systems for recognition of familiar faces. Neuropsychologia. 45: 32-41.

Graham MS, Drobnjak I, Zhang H (2016) Realistic simulation of artefacts in diffusion MRI for validating post-processing correction techniques. Neuroimage. 125: 1079-94.

Grèzes J, Dezecache G (2014) How do shared-representations and emotional processes cooperate in response to social threat signals? Neuropsychologia. 55: 105-14.

Grèzes J, Pichon S, de Gelder B (2007) Perceiving fear in dynamic body expressions. Neuroimage. 35: 959-67.

Grosbras MH, Paus T (2006) Brain networks involved in viewing angry hands or faces. Cereb Cortex. 16: 1087-96.

Hansen CH, Hansen RD (1988) Finding the face in the crowd: an anger superiority effect. J Pers Soc Psychol. 54: 917-24.

Hariri AR, Bookheimer SY, Mazziotta JC (2000) Modulating emotional responses: effects of a neocortical network on the limbic system. Neuroreport. 11:43-8.

Haxby JV, Hoffman EA, Gobbini MI (2002) Human neural systems for face recognition and social communication. Biol Psychiatry. 51: 59-67.

Haxby JV, Ungerleider LG, Horwitz B, Maisog JM, Rapoport SI, Grady CL (1996) Face encoding and recognition in the human brain. Proc Natl Acad Sci. 93: 922-7.

Herrington JD, Taylor JM, Grupe DW, Curby KM, Schultz RT (2011) Bidirectional communication between amygdala and fusiform gyrus during facial recognition. Neuroimage. 56: 2348-55.

Jenkinson M, Smith S (2001) A global optimisation method for robust affine registration of brain images. Med Image Anal. 5: 143-56.

Jenkinson M, Bannister P, Brady M, Smith S (2002) Improved optimization for the robust and accurate linear registration and motion correction of brain images. Neuroimage. 17: 825-41.

Kleinhans NM, Richards T, Sterling L, Stegbauer KC, Mahurin R, Johnson LC, Greenson J, Dawson G, Aylward E (2008) Abnormal functional connectivity in autism spectrum disorders during face processing. Brain. 131: 1000-12.

Koldewyn K, Yendiki A, Weigelt S, Gweon H, Julian J, Richardson H, Malloy C, Saxe R, Fischl B, Kanwisher N (2014) Differences in the right inferior longitudinal fasciculus but no general disruption of white matter tracts in children with autism spectrum disorder. Proc Natl Acad Sci USA. 111: 1981-6.

Korzeniewska A, Kasicki S, Zagrodzka J (1997) Electrophysiological correlates of the limbic-motor interactions in various behavioral states in rats. Behav Brain Res. 87: 69-83.

Krishnan A, Williams LJ, McIntosh AR, Abdi H (2011) Partial Least Squares (PLS) methods for neuroimaging: a tutorial and review. Neuroimage. 56: 455-75.

LaBar KS, Crupain MJ, Voyvodic JT, McCarthy G (2003) Dynamic perception of facial affect and identity in the human brain. Cereb Cortex. 13: 1023-33.

Langner O, Dotsch R, Bijlstra G, Wigboldus DHJ, Hawk ST, van Knippenberg A (2010). Presentation and validation of the Radboud Faces Database. Cognition & Emotion. 24: 1377-88.

Lo LY, Cheng MY (2015) A quick eye to anger: An investigation of a differential effect of facial features in detecting angry and happy expressions. Int J Psychol. doi: 10.1002/ijop.12202. [Epub ahead of print].

Marstaller L, Williams M, Rich A, Savage G, Burianová H (2015) Aging and large-scale functional networks: white matter integrity, gray matter volume, and functional connectivity in the resting state. Neuroscience. 290: 369-78.

McIntosh AR, Bookstein FL, Haxby JV, Grady CL (1996). Spatial pattern analysis of functional brain images using partial least squares. Neuroimage, 3(3), 143-157.

McIntosh AR, Chau WK, Protzner AB (2004). Spatiotemporal analysis of event-related fMRI data using partial least squares. Neuroimage, 23(2), 764-775.

Menon V, Uddin LQ (2010) Saliency, switching, attention and control: a network model of insula function. Brain Struct Funct. 214: 655-67.

Ogawa S, Lee TM, Kay AR, Tank DW (1990). Brain magnetic resonance imaging with contrast dependent on blood oxygenation. Proc Natl Acad Sci. 87: 9868–72.

Patenaude B, Smith SM, Kennedy D, Jenkinson M (2011) A Bayesian model of shape and appearance for subcortical brain. NeuroImage. 56: 907-922.

Phelps EA, LeDoux JE (2005) Contributions of the amygdala to emotion processing: from animal models to human behavior. Neuron. 48: 175-87.

Phelps EA, Ling S, Carrasco M (2006) Emotion facilitates perception and potentiates the perceptual benefits of attention. Psychol Sci. 17: 292-9.

Pichon S, de Gelder B, Grèzes J (2009) Two different faces of threat. Comparing the neural systems for recognizing fear and anger in dynamic body expressions. Neuroimage. 47: 1873-83.

Pichon S, de Gelder B, Grèzes J (2012) Threat prompts defensive brain responses independently of attentional control. Cereb Cortex. 22: 274-85.

Rossion B, Caldara R, Seghier M, Schuller AM, Lazeyras F, Mayer E (2003) A network of occipito-temporal face-sensitive areas besides the right middle fusiform gyrus is necessary for normal face processing. Brain. 126: 2381-95.

Said CP, Haxby JV, Todorov A (2011) Brain systems for assessing the affective value of faces. Philos Trans R Soc Lond B Biol Sci. 366: 1660-70.

Scherf KS, Thomas C, Doyle J, Behrmann M (2014) Emerging Structure–Function Relations in the Developing Face Processing System. Cereb. Cortex. 24(11): 2964-80.

Shaw DJ, Mareček R, Grosbras MH, Leonard G, Bruce Pike G, Paus T (2016) Co-ordinated structural and functional covariance in the adolescent brain underlies face processing performance. Soc Cogn Affect Neurosci. 11: 556-68.

Smith SM (2002) Fast robust automated brain extraction. Hum Brain Mapp. 17: 143-55.

Thomas C, Avidan G, Humphreys K, Jung KJ, Gao F, Behrmann M (2009) Reduced structural connectivity in ventral visual cortex in congenital prosopagnosia. Nat Neurosci. 12: 29-31.

Tournier JD, Calamante F, Gadian DG, Connelly A (2004) Direct estimation of the fiber orientation density function from diffusion-weighted MRI data using spherical deconvolution. Neuroimage. 23: 1176-85.

Tournier JD, Calamante F, Connelly A (2007) Robust determination of the fibre orientation distribution in diffusion MRI: non-negativity constrained super-resolved spherical deconvolution. Neuroimage. 35: 1459-72.

Tournier JD, Calamante F, Connelly A (2010) Improved probabilistic streamlines tractography by 2nd order integration of fiber orientation distributions. Proc. Intl. Soc. Mag. Reson. Med. 18: 1670.

Tournier JD, Calamante F, Connelly A (2012) MRtrix: Diffusion tractography in crossing fiber regions. Int. J. Imaging Syst. Technol. 22: 53–66.

Tsukiura T, Cabeza R (2008) Orbitofrontal and hippocampal contributions to memory for face-name associations: the rewarding power of a smile. Neuropsychologia. 46: 2310-9.

Tzourio-Mazoyer N, Landeau B, Papathanassiou D, Crivello F, Etard O, Delcroix N, Mazoyer B, Joliot M (2002) Automated anatomical labeling of activations in SPM using a macroscopic anatomical parcellation of the MNI MRI single-subject brain. Neuroimage. 15: 273-89.

Veraart J, Sijbers J, Sunaert S, Leemans A, Jeurissen B (2013) Weighted linear least squares estimation of diffusion MRI parameters: strengths, limitations, and pitfalls. NeuroImage. 81: 335-346.

Vuilleumier P, Armony JL, Driver J, Dolan RJ (2003) Distinct spatial frequency sensitivities for processing faces and emotional expressions. Nat Neurosci. 6: 624-31.

Wang X, Zhen Z, Song Y, Huang L, Kong X, Liu J (2016) The Hierarchical Structure of the Face Network Revealed by Its Functional Connectivity Pattern. J Neurosci. 36: 890-900.

Whalen PJ, Shin LM, McInerney SC, Fischer H, Wright CI, Rauch SL (2001) A functional MRI study of human amygdala responses to facial expressions of fear versus anger. Emotion. 1: 70-83.

Williams LM, Phillips ML, Brammer MJ, Skerrett D, Lagopoulos J, Rennie C, Bahramali H, Olivieri G, David AS, Peduto A, Gordon E (2001) Arousal dissociates amygdala and hippocampal fear responses: evidence from simultaneous fMRI and skin conductance recording. Neuroimage. 14: 1070-9.

Figure Captions:

Figure 1: Behaviour and white matter integrity. A: Mean reaction times (+/- SEM) show significantly slower responses when matching angry and fearful facial expressions than when matching shapes. B: Mean fractional anisotropy (FA) values (+/- SEM) for left and right inferior longitudinal fasciculus (left). Tractography results from a representative subject (right).

Figure 2: Whole-brain activity differentiating faces and shapes. Warm colours show functional activity in posterior parietal cortices during processing of shapes. Cool colours depict functional activity in the core and extended emotional face processing regions, including inferior occipital gyrus, fusiform gyrus, and dorsal amygdala, during processing of angry and fearful facial expressions.

Figure 3: Whole-brain activity contrasting angry and fearful facial expressions. Warm colours show functional activity related to angry facial expressions. Cool colours depict functional activity related to fearful facial expressions.

Figure 4: Individual differences in the three-way relation between behaviour, functional connectivity, and ILF white matter integrity for angry faces. Left: Whole-brain patterns showing functional connectivity with the right amygdala negatively correlated with reaction times and positively with ILF FA values, including hippocampus, brainstem, and the right temporal pole. Right: Scatter plots demonstrate correlations between individual PLS brain scores (indicating how strongly each individual expressed the whole-brain pattern) on the ordinate and the covariates

reaction time (in msec), left and right amygdala functional seeds (in % signal change), as well as mean FA values of left and right ILF (in arbitrary units) on the abscissa.

Figure 5: Three-way relation between behaviour, functional connectivity, and ILF white matter integrity for fearful faces. Left: Whole-brain patterns showing functional connectivity with the right amygdala correlated with reaction times and ILF FA values, including bilateral lingual gyrus, precuneus, middle and superior frontal gyrus, supramarginal gyrus, and precentral gyrus. Right: Scatter plots demonstrate correlations between individual PLS brain scores (indicating how strongly each individual expressed the whole-brain pattern) on the ordinate and the covariates reaction time (in msec), left and right amygdala functional seeds (in % signal change), as well as mean FA values of left and right ILF (in arbitrary units) on the abscissa.

Figure 1
Click here to download high resolution image

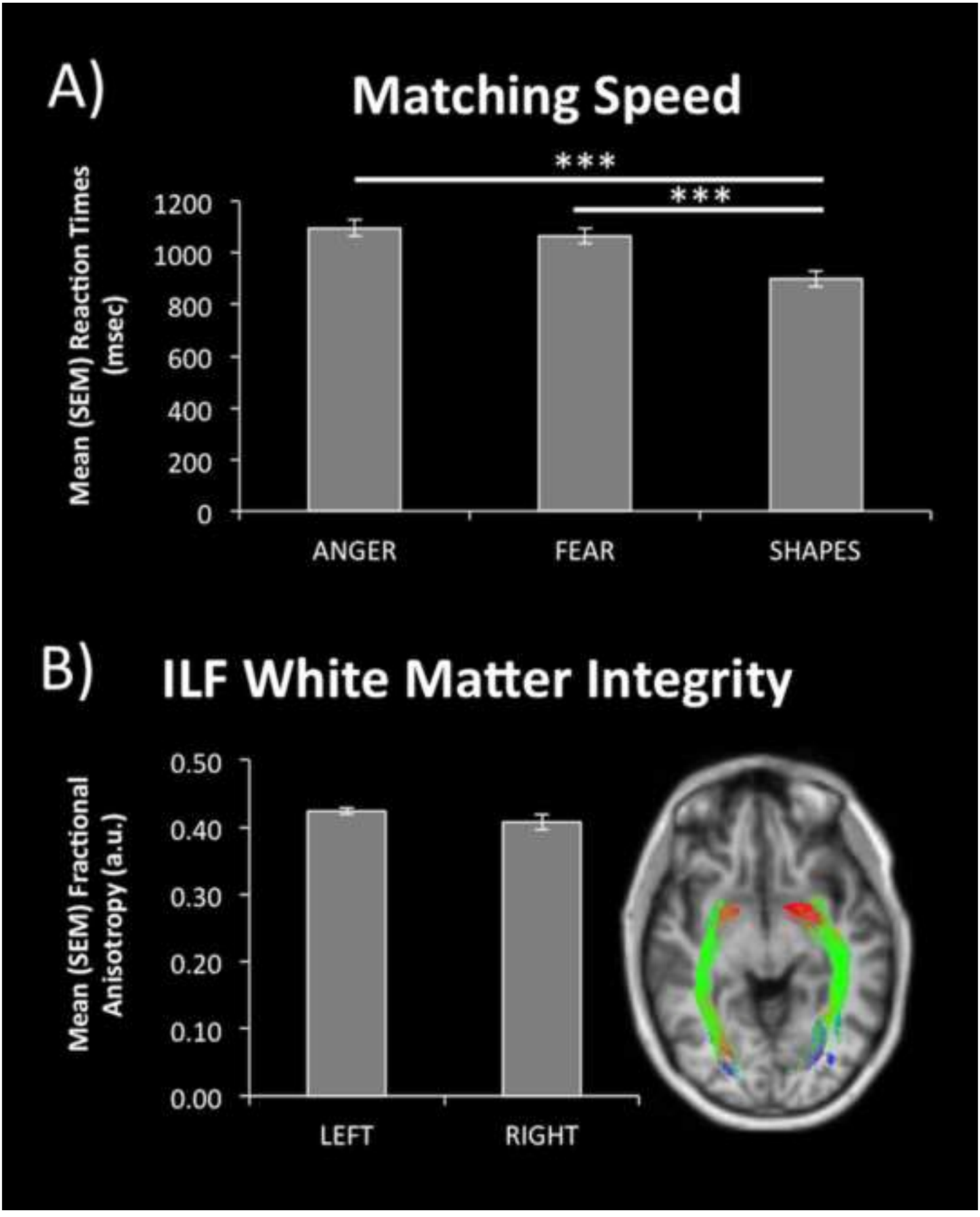

Figure 2
Click here to download high resolution image

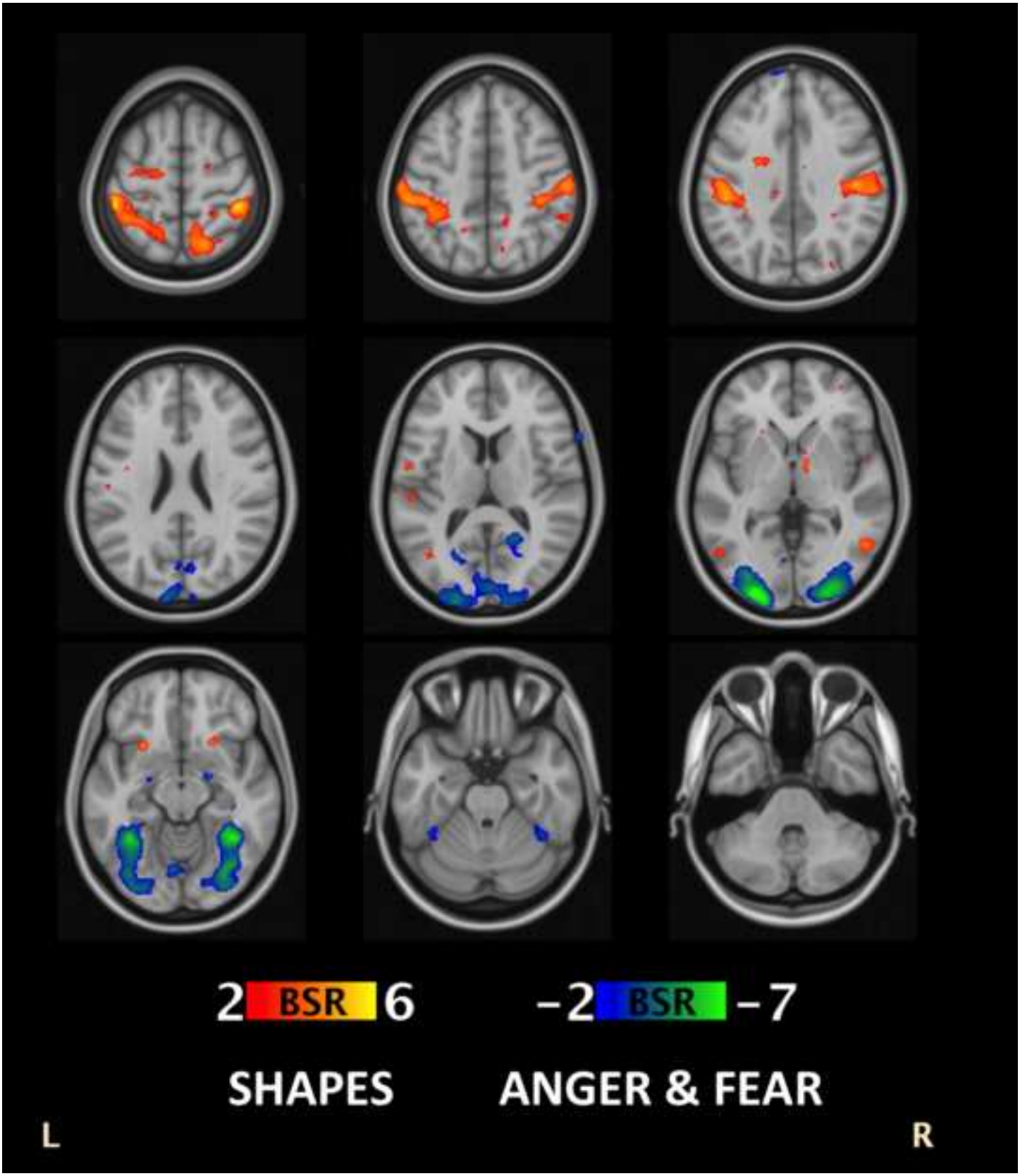

Figure 3
Click here to download high resolution image

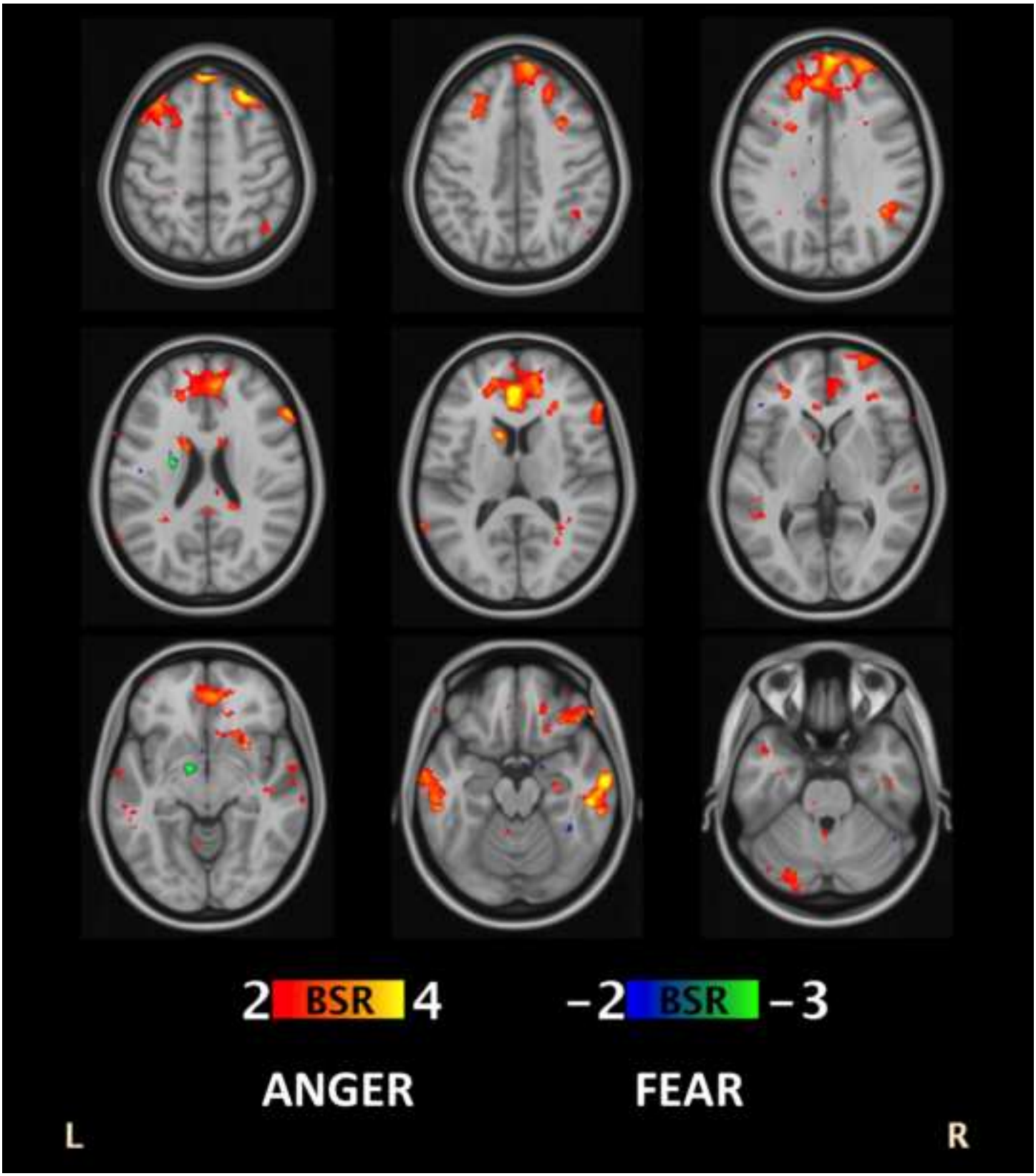

Figure 4

Click here to download high resolution image

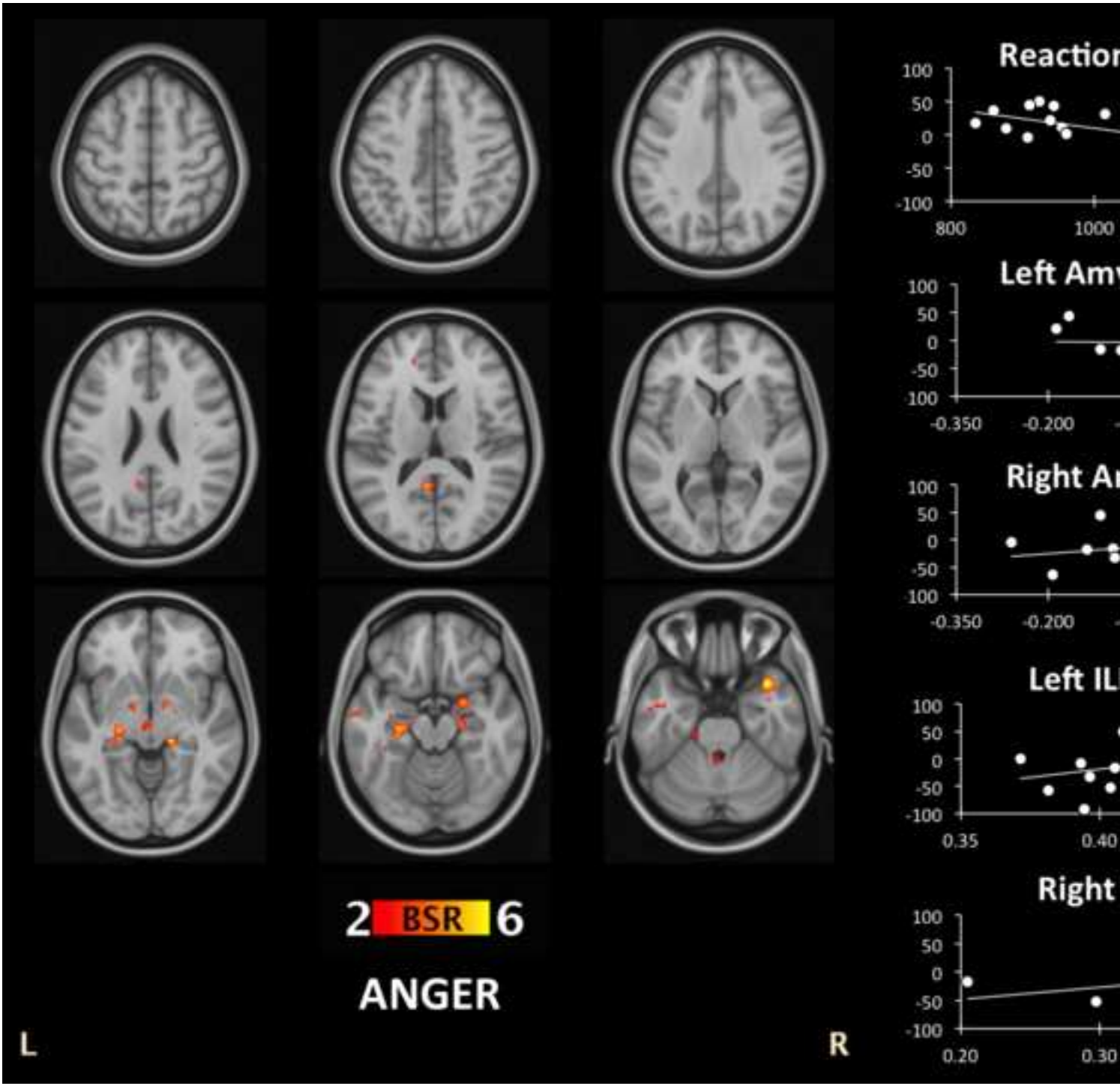

Figure 5

Click here to download high resolution image

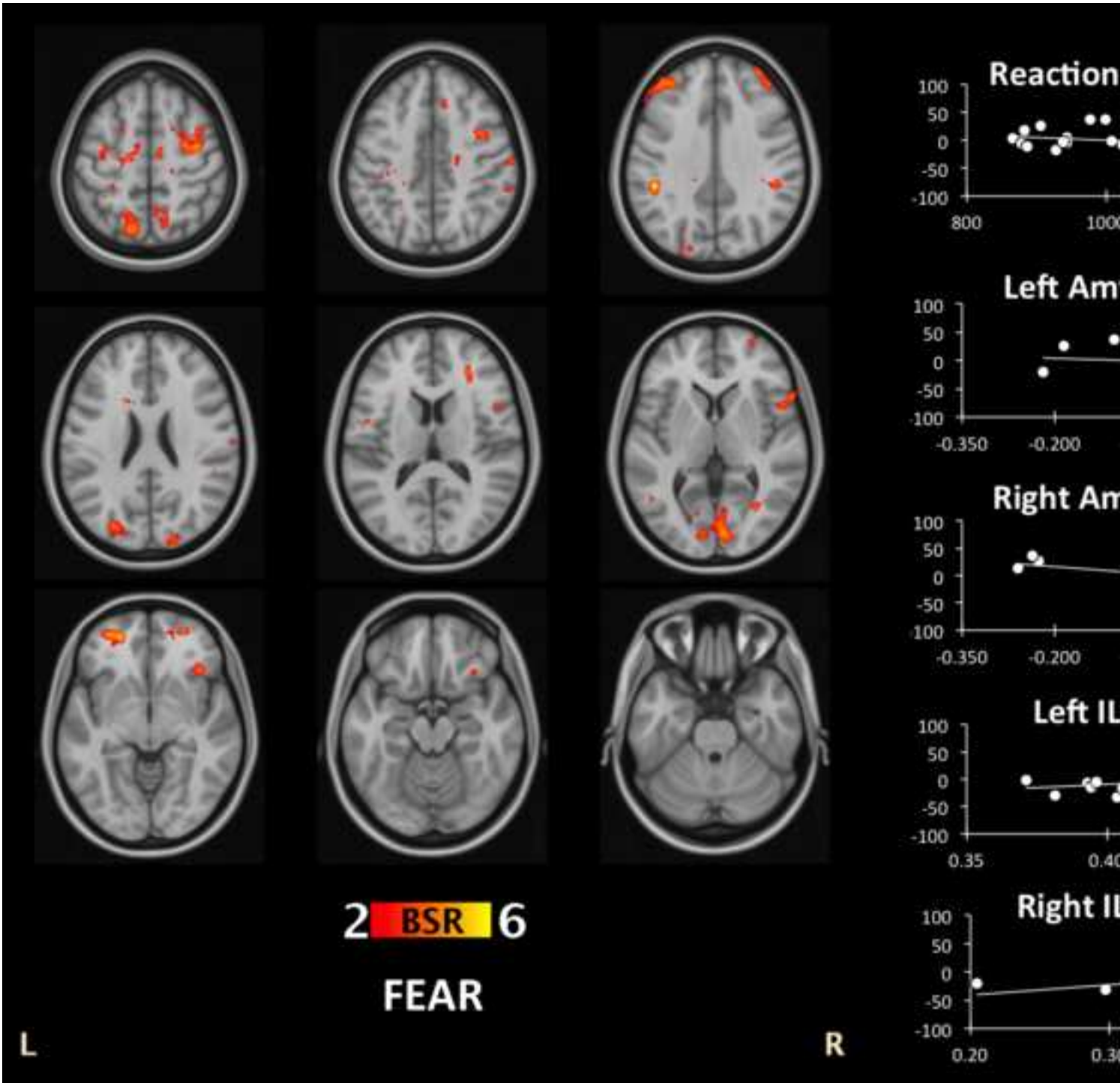

Table 1

Table 1: MNI coordinates of peak voxels of whole-brain results differentiating shapes from angry and fearful face processing.

Region	Hem	MNI Coordinates			Ratio
		x	*y*	*z*	
Shapes > Angry & Fearful Faces					
Postcentral gyrus	L	-42	-36	54	6.1
	R	44	-36	64	7.6
Superior parietal lobule	L	-26	-46	56	6.7
Angry & Fearful Faces > Shapes					
Amygdala	L	-20	-8	-12	-4.0
	R	22	-6	-12	-4.3
Fusiform gyrus	L	-34	-50	-14	-6.8
	R	38	-46	-20	-9.4
Superior occipital cortex	L	-24	-94	0	-8.3
	R	28	-94	4	-8.1

Table 2

Table 2: MNI coordinates of peak voxels of whole-brain results differentiating angry from fearful face processing.

Region	Hem	MNI Coordinates			Ratio
		x	*y*	*z*	
Angry > Fearful Faces					
Middle frontal gyrus	L	-30	32	50	3.7
	R	28	34	52	5.0
Ventrolateral prefrontal cortex	R	56	26	16	4.0
Frontal orbital cortex	R	32	30	-16	3.6
Anterior cingulate cortex	L	-2	42	10	4.8
Supramarginal gyrus	R	42	-48	34	3.4
Middle temporal gyrus	L	-64	-8	-18	3.4
	R	64	-14	-16	5.3
Caudate	L	-10	12	10	4.3
Fearful > Angry Faces					
Amygdala	R	18	-4	-18	-2.5
Pallidum	L	-12	-4	-6	-4.0
Fusiform gyrus	R	38	-46	-18	-2.3